Chapter 7
Modeling and Analysis of Ventricular Response in Atrial Fibrillation

Valentina D. A. Corino, Frida Sandberg, Luca T. Mainardi and Leif Sörnmo

7.1 Introduction

The ventricular response in atrial fibrillation (AF) is highly irregular, mainly due to the atrial impulses arriving irregularly at the atrioventricular (AV) node. As a result, the RR intervals differ dramatically in length. Despite the irregularity, the ventricular response is not completely random, but exhibits weak correlation [1] and certain short- or long-term predictability [2]. Another characteristic is that the ventricular rate is often higher in AF than in normal sinus rhythm, a characteristic explored in AF detection, see Chap. 4. The RR interval series observed in normal sinus rhythm and AF differ with respect to both variability and irregularity, two aspects which are illustrated in Fig. 7.1.

The ventricular response plays a significant role in the management of patients with AF [3]. In fact, the control of ventricular rate effectively reduces the risk of complication and improves the quality of life. Therefore, the study of factors influencing ventricular rate and its dynamics is of great importance as it may lead to strengthened decision-making in AF management.

To characterize normal sinus rhythm, a wide range of parameters have been investigated, often categorized into dispersion parameters to characterize RR variability,

V. D. A. Corino · L. T. Mainardi
Department of Electronics, Information and Bioengineering, Politecnico di Milano,
Milan, Italy
e-mail: valentina.corino@polimi.it

L. T. Mainardi
e-mail: luca.mainardi@polimi.it

F. Sandberg · L. Sörnmo (✉)
Department of Biomedical Engineering and Center for Integrative Electrocardiology,
Lund University, Lund, Sweden
e-mail: leif.sornmo@bme.lth.se

F. Sandberg
e-mail: frida.sandberg@bme.lth.se
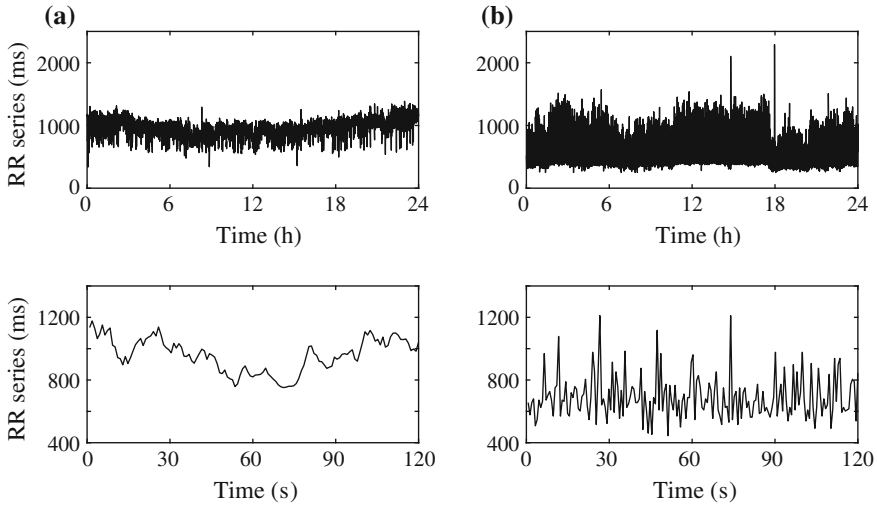
Fig. 7.1 24-h RR interval series in **a** normal sinus rhythm and **b** AF. The 24-h plots (top row) show that the dispersion is much larger in AF than in normal sinus rhythm. The zoomed-in segments (bottom row) demonstrate that the RR interval series in AF not only has larger dispersion, but it is also much more irregular

spectral parameters to characterize autonomic influence on the sinus node, and different types of entropy to characterize RR irregularity. To characterize AF, spectral parameters have received very limited interest since the RR interval spectrum is essentially flat, and lacks peaks which may carry physiological information [4]. On the other hand, dispersion parameters and entropy measures have conveyed clinically valuable information: for example, lower variability and/or irregularity of the RR interval series have been associated with poor outcome in patients with AF [5, 6]. Given the growing clinical interest to understand the characteristics of the RR intervals, an overview of results reported in clinical studies is provided in Sect. 7.2.

The analysis of ventricular response can be augmented with information on f waves so that the coupling between the atria and the ventricles, through the AV node, can be investigated. The AV node plays a particularly important role in AF by acting as a "filter" which blocks certain atrial impulses, with repercussions on ventricular activation. By developing methods for analyzing AV nodal properties, patient-specific information may be obtained which describes the effect of a certain antiarrhythmic drug. The properties can be studied by means of mathematical modeling, considered either for simulation of various scenarios or estimation of model parameters. In the latter case, the observed signal is acquired either invasively or from the surface ECG. Signal processing techniques are usually required to separate the atrial from the ventricular activity before parameter estimation can be performed, see Chap. 5.

Section 7.3 provides a brief overview of methods for heuristic assessment of the AV node. Section 7.4 describes a method for analyzing the relationship between

atrial input and ventricular response during AF. Sections 7.5 and 7.6 review several AV node models for simulation and parameter estimation, respectively. The chapter concludes with a comparison of AV node models in Sect. 7.7.

7.2 RR Interval Analysis

Classical dispersion parameters such as the coefficient of variation and the root mean square of successive differences (RMSSD), defined in (4.2) and (4.3), respectively, have been found useful for characterizing the variability of RR intervals in AF [2, 7].[1] However, variability parameters provide an incomplete characterization of RR intervals, since they cannot characterize irregularity, i.e., the degree of unpredictability. Therefore, variability parameters have been complemented with different entropy measures to characterize irregularity, including approximate entropy I_{ApEn}, sample entropy I_{SampEn}, and Shannon entropy I_{ShEn} (see Sect. 4.2.1 for definitions), as well as conditional entropy [8]. Figure 7.2 illustrates the difference between variability
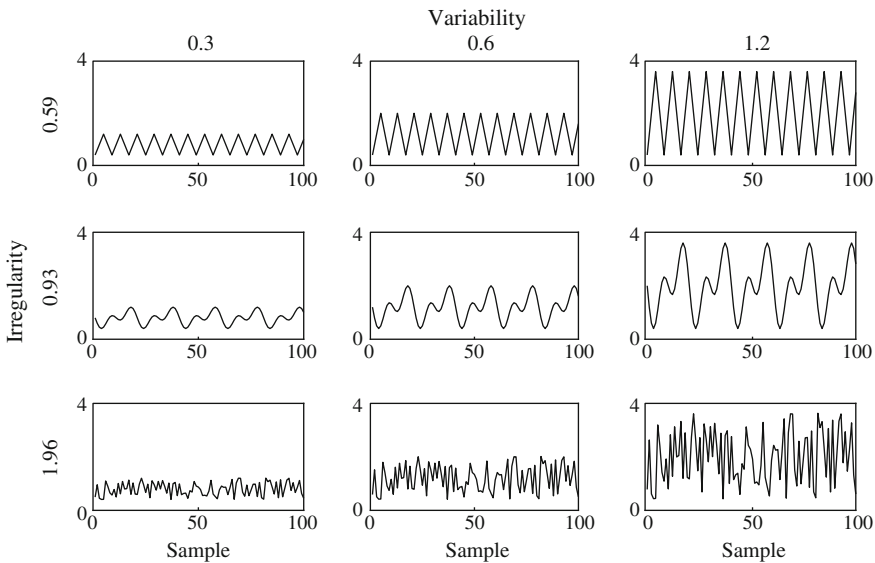
Fig. 7.2 Illustration of the difference between variability, quantified by the standard deviation, and irregularity, quantified by the sample entropy. Each row shows a time series with identical irregularity (given by the numbers to the left of the diagrams), but increasing variability from left to right, whereas each column shows series with identical variability (given by the numbers on above the diagrams), but increasing irregularity from top to bottom. The units of the horizontal and vertical axes are arbitrary

---

[1]The reason for not using the term "ventricular response" in this section is that it implies, at least in this book, that an atrial input is also part of the analysis.

and irregularity for different time series with identical variability but different irregularity, and vice versa.

Two early studies analyzed the RR interval series in patients with AF, demonstrating that reduced variability is associated with worse outcome [5, 6]. Using the 24-h ambulatory ECG, reduced RR interval irregularity was found to have independent prognostic value for cardiac mortality during long-term follow-up in patients with permanent AF [9].

The association between RR intervals and long-term clinical outcome has been evaluated in a population of ambulatory patients with mild-to-moderate heart failure and AF at baseline. Patients with symptomatic heart failure were enrolled in a multicenter study on sudden death [10]. Both I_{ApEn} and I_{ShEn} were found to be significantly lower in nonsurvivors than in survivors for all subgroups of death (total mortality, sudden death, and heart failure death). Patients with a lower I_{ApEn} had significantly lower survival: Kaplan–Meier analysis [11] showed that a lower I_{ApEn} was associated with a nearly fourfold higher total mortality (40% vs. 12%) and more than six times higher mortality due to progression of heart failure (19% vs. 3%) and sudden death (18 vs. 3%). The criterion $I_{ApEn} < 1.68$, where 1.68 is the lower tertile of the data set, was found to be a significant predictor of all types of mortality after adjustment for significant clinical covariates [12], leading up to the main finding that lower irregularity is associated with worse outcome in AF patients.

Results in the literature suggest that irregularity parameters may be used as risk indicators. Thus, it is of interest to investigate to what extent irregularity is affected by commonly used rate-control drugs. The effect of the selective A1-receptor agonist tecadenoson, alone as well as in combination with the beta blocker esmolol, was assessed in a small group of AF patients [13]. Tecadenoson was found to reduce heart rate and increase variability, but did not have any effect on irregularity. Beta blockade with intravenous esmolol further increased variability and decreased heart rate. In another study [14], no significant differences in RR irregularity, as quantified by I_{ApEn}, were observed in patients with AF and congestive heart failure when treated with beta blockers, digoxin, or amiodarone. The effect of rate-control drugs on RR variability/irregularity was investigated in 60 patients with permanent AF, involving the drugs diltiazem, verapamil (both calcium channel blockers), metoprolol, and carvedilol (beta blocker) [15]. Variability was assessed by well-known parameters such as the standard deviation and the RMSSD, whereas irregularity was assessed by I_{ApEn}, I_{ShEn}, and a measure based on conditional entropy [16]. A significantly lower heart rate was obtained for all investigated drugs, reaching its lowest rate for the calcium channel blockers. Moreover, all drugs were found to increase RR variability significantly relative to the baseline recording, whereas only the beta blockers increased RR irregularity significantly.

Using the data set in [15], circadian variation was investigated by means of five ambulatory recordings per patient, obtained at baseline as well as during the four different drug regimens [17]. Variability and irregularity parameters were computed in nonoverlapping, 20-min segments. Circadianity was assessed using cosinor analysis of the resulting series, characterized by the 24-h mean and the excursion over the mean described by the amplitude of the cosine fitted to the data [18]. Heart rate and

variability parameters, including the standard deviation and the RMSSD, exhibited significant circadian variation in most patients, whereas circadian variation in I_{ApEn} and I_{SampEn} was detected in only a few patients. When circadian variation was detected in I_{ApEn} at baseline, the patients had more severe symptoms. All drugs decreased the rhythm-adjusted mean of the heart rate and increased the rhythm-adjusted mean of variability parameters (the rhythm-adjusted mean is also referred to as "midline estimating statistic of rhythm", MESOR [19]). Only carvedilol and metoprolol decreased the normalized amplitude over the 24 h of the irregularity parameters and heart rate. The results suggested that circadian variation can be observed in most patients using variability parameters, but only in a few patients using irregularity parameters.

The above-mentioned clinical studies are limited by small patient groups. Therefore, further studies are needed to better assess whether variability and irregularity parameters are predictive of patient status.

7.3 Heuristic Assessment of the Atrioventricular Node

Rate-control drugs act on atrial and/or AV nodal properties to lower the ventricular rate. During drug development, electrophysiological effects of antiarrhythmic drugs are usually assessed invasively in sinus rhythm. Since an atrial pacing protocol cannot be applied in patients with AF, the electrophysiological drug effects on the AV node are still not completely understood. When optimizing drug therapy, noninvasive assessment of AV nodal electrophysiology may help to select optimal therapy. During the early clinical phases of drug development, noninvasive characterization of the AV node may facilitate data collection from large patient cohorts and favor patient-tailored therapy. Estimation of the AV nodal refractory period using the surface ECG has been attempted in several studies, employing different heuristic approaches [20–24].

Heuristic assessment of AV nodal electrophysiology has relied on simple approaches to characterizing the RR intervals. Noninvasive estimation of the functional refractory period of the AV node during AF has been attempted by simply selecting the shortest RR interval or the 5-th percentile of the RR interval series [20, 23, 25]. In dogs, it was demonstrated that the shortest RR interval correlated statistically with the functional refractory period, determined using a pacing protocol. Therefore, the shortest RR interval was used as a surrogate measurement of the functional refractory period [20].

Using the Poincaré plot, where each RR interval is plotted against the preceding RR interval, an estimate of the functional refractory period can be obtained as well. The value of the lower envelope, determined as a regression line, at 1 s ("1 s intercept") and the degree of scatter above the lower envelope have been proposed as surrogate measurements of AV nodal refractoriness and concealed AV conduction, i.e., the effect of blocked impulses on the conduction of subsequent impulses, respectively. The circadian variation of the 1-s intercept of the lower envelope was investigated in 120 patients who underwent 24-h ambulatory monitoring at baseline [24]. During

an observation period of 33 ± 16 months, there were 25 deaths, including 13 cardiac and 8 stroke deaths. All patients showed significant circadian rhythms in the lower envelope, however, patients dying subsequently from cardiac causes, but not from fatal stroke, had less pronounced circadian rhythm, with amplitudes which were less than 55% of those in surviving patients. It was suggested that blunted circadian rhythm of AV conduction represents an independent risk of cardiac death in patients with permanent AF.

The presence of clusters in the histogram-based Poincaré plot, based on the RR intervals derived from the 24-h ambulatory ECG, has been suggested as a marker of higher AF organization to predict the outcome of electrical cardioversion [26]. A cluster was considered to be present when a peak in the histogram plot could be identified visually. Later, the histogram-based Poincaré plot served as the basis for the Poincaré surface profile, i.e., a univariate histogram defined by those RR intervals which are preceded by RR intervals of approximately the same length [27], cf. Sect. 4.2.2. The Poincaré surface profile was proposed as a tool for characterizing AV nodal memory effect and detecting preferential AV nodal conduction. However, neither the Poincaré plot nor the histogram-based Poincaré plot analysis have raised much interest in the research community. This may be due to a number of reasons, including that the plot is strongly dependent on bin size, the bins must be sufficiently well-populated with points to produce meaningful results, and manual interaction is often needed to determine the lower envelope [24].

7.4 Synchrogram Analysis

Synchrogram analysis has been introduced for exploratory analysis of the relationship between atrial input and ventricular response during AF, providing valuable insights into AV nodal function [28]. The method is purely phenomenological, and no attempt is made to account for AV nodal electrophysiological properties such as refractoriness and conduction delay. The analysis is applied to atrial activations, determined from the electrogram, and ventricular activations, determined from the ECG, to analyze AV coupling. The analysis is performed by observing the phase of the ventricular activations at time instants triggered by the atrial activations. The instantaneous ventricular phase is assumed to be a monotonically increasing, piecewise linear function, defined by

$$\phi_v(t) = 2\pi \frac{t - t_{v,n-1}}{t_{v,n} - t_{v,n-1}} + 2\pi n, \quad t_{v,n-1} \le t < t_{v,n}, \quad n = 0, \ldots, N-1, \quad (7.1)$$

where $t_{v,n}$ is the time of n-th ventricular activation and N is the total number of ventricular activations. To be consistent with the indexing of RR intervals adopted in Chap. 4, the first RR interval, defined by $x_0 = t_{v,0} - t_{v,-1}$, requires that the time of the first ventricular activation is indexed by -1.

The instantaneous ventricular phase is normalized to the interval $[0, q]$, and sampled at the time of atrial activations $t_{a,k}$ for the purpose of detecting whether $p : q$ coupling is present,

$$\Psi_q(t_{a,k}) = \frac{1}{2\pi}\left(\phi_v(t_{a,k}) \bmod (2\pi q)\right), \quad q = 1, 2, 3, \qquad (7.2)$$

where p is the number of atrial activations and q is the number of ventricular activations. Epochs of synchronization are automatically detected by alternately dividing the values of $\Psi_q(t_{a,k})$ into different subgroups. The normalized phases are classified as $p : q$ coupling whenever the absolute difference between $\Psi_q(t_{a,k+p})$ and $\Psi_q(t_{a,k})$ within a subgroup is below a predefined tolerance threshold. The synchrogram analysis is illustrated in Fig. 7.3.

The synchrogram was investigated in both atrial flutter and AF. As expected, the percentage of coupled beats and the duration of coupled epochs were significantly
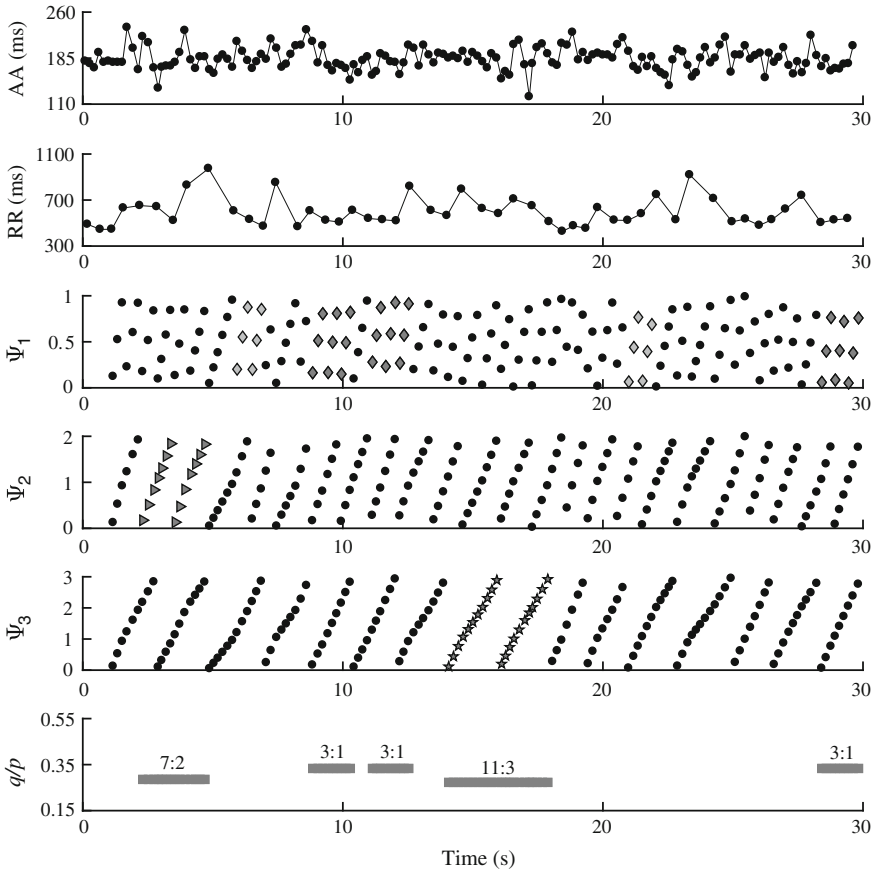
Fig. 7.3 AV synchrogram analysis of AF [28]. Atrial-to-atrial (AA) and RR interval series, normalized instantaneous ventricular phases $\Psi_1(t_{a,k})$, $\Psi_2(t_{a,k})$, $\Psi_3(t_{a,k})$, defined in (7.2), and ratio of ventricular to atrial activations q/p of the synchronized epochs (top to bottom). Note that $p : q$ is displayed inside the bottom diagram, whereas the ratio q/p is the unit of the vertical axis. (Modified from [28] with permission.)

higher in atrial flutter than in AF [28]. Moreover, the synchrogram was used to assess the dynamics of AV coupling as a function of atrial fibrillatory rate (AFR) in a small group of patients during spontaneous acceleration of the AFR at the onset of an AF episode; in this particular assessment, the AFR was estimated from the electrogram. The results demonstrated that the occurrence and the duration of coupled epochs decreased as the AFR increased, and that the average AV conduction ratio, i.e., the ratio of ventricular to atrial activations, was significantly smaller at higher AFRs [29].

Synchrogram analysis has also been considered for investigating the effects of atrial activity and AV nodal conduction on the ventricular response in patients with paroxysmal AF [30]. The results showed that ventricular rate and RR variability are significantly correlated with the average AV conduction ratio and the variability of the atrial input. On the other hand, the AFR is not correlated with ventricular rate nor with RR variability.

7.5 Mathematical Modeling of the Atrioventricular Node

Refractoriness and concealed conduction of the AV node are important AV nodal properties which contribute to forming the ventricular response. Due to refractoriness, many atrial impulses are blocked when arriving to the AV node. Concealed conduction of a single atrial impulse, occurring when the impulse only partially penetrates into the AV node without reaching the ventricles, influences the conduction of subsequent atrial impulses. Moreover, the existence of two dominant pathways through the AV node, each with its own electrophysiological properties, is well-documented and plays an important role in AF.

The properties of AV nodal function can be studied by mathematical modeling which may be categorized into:

- Models primarily developed for simulation to provide better understanding of AV nodal properties, sometimes involving intracardiac information on atrial activity where the arrival times of the atrial impulses are known (this section).
- Models primarily developed for statistical estimation of AV node parameters, relying entirely on information derived from the surface ECG. The arrival times of atrial impulses are modeled as a random process (Sect. 7.6).

7.5.1 Modeling of Conduction Delay in Non-AF Rhythms

Conduction delay is an important AV nodal property, and has therefore received considerable attention in mathematical model building. With reference to AV nodal conduction in Wenckebach periodicity, i.e., a non-AF rhythm, the conduction delay d_k related to the k-th atrial impulse depends on the AV nodal recovery time (RT) $\Delta t_{RT,k}$. The conduction delay is modeled by [21]

$$d_k = d_{\min} + \alpha_{\max} \exp\left[-\frac{\Delta t_{\mathrm{RT},k}}{\gamma_c}\right], \tag{7.3}$$

where $d_{\min}$ is the minimal conduction delay, $\alpha_{\max}$ is the maximal prolongation of the conduction delay, and γ_c is the time constant of the exponential conduction curve. The recovery time $\Delta t_{\mathrm{RT},k}$ is given by the time elapsing from the preceding ventricular activation $t_{v,n}$ to the current AV nodal activation time $t_{a,k}$,

$$\Delta t_{\mathrm{RT},k} = t_{a,k} - t_{v,n}, \quad t_{a,k} > t_{v,n}, \tag{7.4}$$

where ventricular activations are indexed by n.

The basic model of conduction delay in (7.3) can be expanded to include rate-dependent shortening of the conduction delay, referred to as *facilitation* (fac), and rate-dependent prolongation of the recovery time, referred to as *fatigue* (fat) [21], see also [31]. In the expanded model, the conduction delay d_k in (7.3) is denoted d_k', $\alpha_{\max}$ is replaced by α_k to model facilitation, and the term s_k is introduced to model fatigue,

$$d_k' = d_{\min} + s_k + \alpha_k \exp\left[-\frac{\Delta t_{\mathrm{RT},k}}{\gamma_c}\right]. \tag{7.5}$$

Facilitation is incorporated into the model by assuming that the maximal prolongation $\alpha_{\max}$ depends on the interval $\Delta t_{a,k-1}$ between two successive atrial impulses immediately preceding $t_{a,k}$, commonly referred to as the AA interval,

$$\alpha_k = \alpha_{\max} - \kappa \exp\left[-\frac{\Delta t_{a,k-1}}{\gamma_{\mathrm{fac}}}\right], \tag{7.6}$$

where

$$\Delta t_{a,k} = t_{a,k} - t_{a,k-1}, \tag{7.7}$$

and $\alpha_{\max}$, γ_{fac}, and κ are model constants. Fatigue is incorporated by assuming that each AV nodal activation causes a slowing of the conduction delay of all subsequent impulses, modeled by

$$s_k = s_{k-1} \exp\left[-\frac{\Delta t_{a,k-1}}{\gamma_{\mathrm{fat}}}\right] + \eta \exp\left[-\frac{\Delta t_{\mathrm{RT},k}}{\gamma_{\mathrm{fat}}}\right], \tag{7.8}$$

where η and γ_{fat} are model constants.

The conduction delay model, defined by (7.3)–(7.8), was fitted to experimental data obtained from seven autonomically blocked dogs during pacing [21]. The results showed that the model can accurately predict dynamic changes in Wenckebach periodicity. Although the model does not account for concealed conduction, it has nonetheless served as a starting point for AV node modeling in AF [32–35].

7.5.2 Modeling of Conduction Delay in AF

An AV node model accounting for conduction delay, defined by (7.3), and refractoriness in AF was proposed in [33, 34], however, fatigue and facilitation were not modeled. In that model, the AV node becomes refractory after an atrial impulse has been conducted through the AV node to the ventricles. Impulses arriving to the AV node during the refractory period are blocked (concealed), and each blocked impulse causes the refractory period to be prolonged, first with a fixed length [33], but later with a Gaussian random variable [34].

The proposed model, with fixed prolongation of the refractory period, was tested on one, single intracardiac recording from a patient with AF, exhibiting an agreement between the estimated and the observed RR series which is not particularly satisfactory, see Fig. 7.4. Using instead the model with random prolongation [34], a better fit was obtained. The significance of these two conduction delay models remain to be established on a larger set of data.

More recently, a dual-pathway AV node model has been proposed in which the conduction delay, similar to the model in [21], is assumed to be affected by the stimulation history [36]. The conduction delay is described by the model in (7.3), except that $\alpha_{\max}$ and γ_c are assumed to be functionally dependent on the preceding conduction delay d_{k-1},
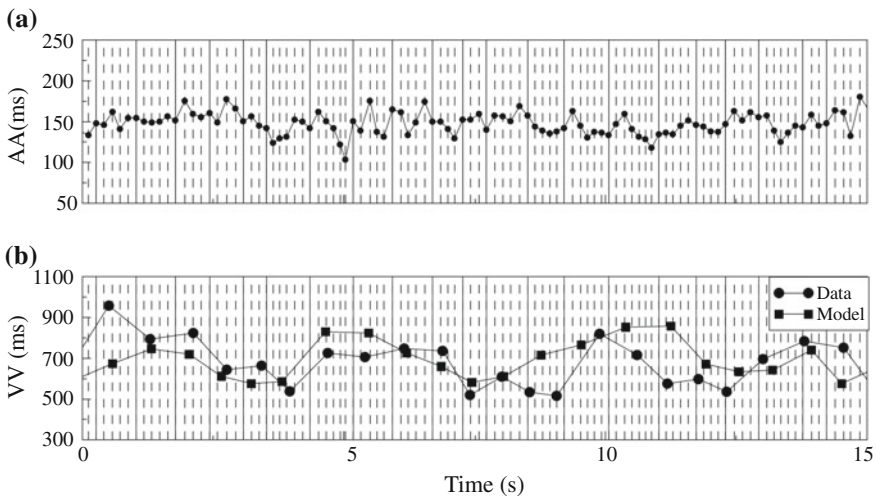
Fig. 7.4 **a** Atrial-to-atrial (AA) and **b** ventricular-to-ventricular (VV) intervals obtained from an intracardiac recording. Ventricular-to-ventricular intervals were obtained using the AV node model in [33]. The vertical lines in both panels are the times of the atrial impulses, where vertical, solid lines indicate conducted impulses, and vertical, dashed lines indicate blocked impulses. (Reprinted from [33] with permission)

$$\alpha_{\text{max},k} = a_1 d_{k-1}^2 + a_2 d_{k-1} + a_3, \tag{7.9}$$

and

$$\gamma_{\text{c},k} = b_1 + \left(\frac{d_{k-1}}{b_2}\right)^{b_3}, \tag{7.10}$$

respectively. The model constants a_1, a_2, a_3, b_1, b_2, and b_3 are assumed to differ between the two pathways. Concealed conduction is modeled by a virtual conduction delay $\tilde{d}_k$ which depends on the AA interval $\Delta t_{a,k}$ [36],

$$\tilde{d}_k = c_1 - c_2 \exp\left[-\frac{\Delta t_{a,k}}{c_3}\right], \tag{7.11}$$

implying that $\Delta t_{\text{RT},k}$ in (7.3) is replaced by $(\Delta t_{a,k} - \tilde{d}_{k-1})$,

$$d_k = d_{\min} + \alpha_{\text{max},k} \exp\left[-\frac{(\Delta t_{a,k} - \tilde{d}_{k-1})}{\gamma_{c,k}}\right]. \tag{7.12}$$

The model constants c_1, c_2, and c_3 are assumed to differ between the two pathways. It should be noted that the effect of replacing $\Delta t_{\text{RT},k}$ by $(\Delta t_{a,k} - \tilde{d}_{k-1})$ is similar to that of prolongation of the refractory period due to concealed conduction, see Sect. 7.5.4.

The model parameters were estimated by fitting $\alpha_{\text{max},k}$ and $\gamma_{c,k}$ to data obtained using a pacing protocol. The fitted model could predict the conducting pathway with specificity and sensitivity exceeding 85% when AF-like random stimulation was applied to a rabbit preparation. His' electrogram alternans was used to determine the pathway of each conducted impulse in the experimental data [37].

7.5.3 Modeling of Refractory Period in AF

In a simple model accounting for the refractory period, the atrial impulses are assumed to arrive randomly in time at the AV node according to a Gaussian distribution [38]. Each atrial impulse results in ventricular activation, unless the AV node is refractory which causes the atrial impulses to be blocked and the refractory period to be prolonged. For each blocked atrial impulse, the refractory period τ_k, following the k-th atrial impulse arriving at the AV node after ventricular activation, is prolonged according to the following equation:

$$\tau_{k+1} = \tau_k + u_k(0.9 - \tau_k), \quad k \geq 0. \tag{7.13}$$

The time-dependent prolongation u_k of the refractory period is described by the logistic function

$$u_k = \frac{1}{1 + e^{-a(z_k - b)}}, \tag{7.14}$$

where

$$z_k = 1 - \frac{t_{a,k}}{\tau_k}, \quad \tau_k > t_{a,k}, \tag{7.15}$$

and a and b are positive-valued model constants. The index k is reset to 0 and τ_0 is reset to 0.3 s when a ventricular activation occurs [38]. The parameters a and b define the shape of the RR interval histogram, but lack a physiological interpretation. For the model in (7.13)–(7.15), an atrial impulse arriving close in time to a conducted atrial impulse prolongs the refractory period more than an atrial impulse arriving at the end of the refractory period. The blocked atrial impulses prolong the refractory period τ_k towards its upper limit of 0.9 s.

7.5.4 Modeling of Refractory Period and Conduction Delay in AF

A much more sophisticated AV node model for the simulation of ventricular activation during AF was proposed in [35, 39], see also [40, 41], where conduction delay, prolongation of the refractory period due to concealed conduction, and ventricular pacing (VP) are also taken into account. The AV node is activated due to the combined effect of spontaneous depolarization and AF bombardment. However, the AV node can also be activated by a VP-induced, retrograde wave. The activation initiates a refractory period during which the AV node is nonresponsive to atrial impulses as well as to a VP-induced retrograde wave. When the refractory period ends, the transmembrane potential returns to its resting potential and initiates a spontaneous, linear increase in the transmembrane potential. Each time an AF impulse arrives at the AV node when not being in a refractory state, its transmembrane potential is increased by a discrete amount, see Fig. 7.5. If instead a VP-induced retrograde wave penetrates the AV node in a nonrefractory state, the transmembrane potential reaches its threshold immediately.

In this model, the conduction delay d_k is modeled by (7.3), and the refractory period τ_k is modeled by

$$\tau_k = \tau_{\min} + \beta \left(1 - \exp\left[-\frac{\Delta t_{\text{RT},k}}{\gamma_r} \right] \right), \tag{7.16}$$

where $\tau_{\min}$ is the shortest refractory period, β is the maximal prolongation of the refractory period, and γ_r is the time constant of the exponential refractory curve. Moreover, the model accounts for prolongation of the refractory period due to concealed conduction. The prolonged refractory period is a product of two factors: one depending on the arrival time of the atrial impulse and another depending on the
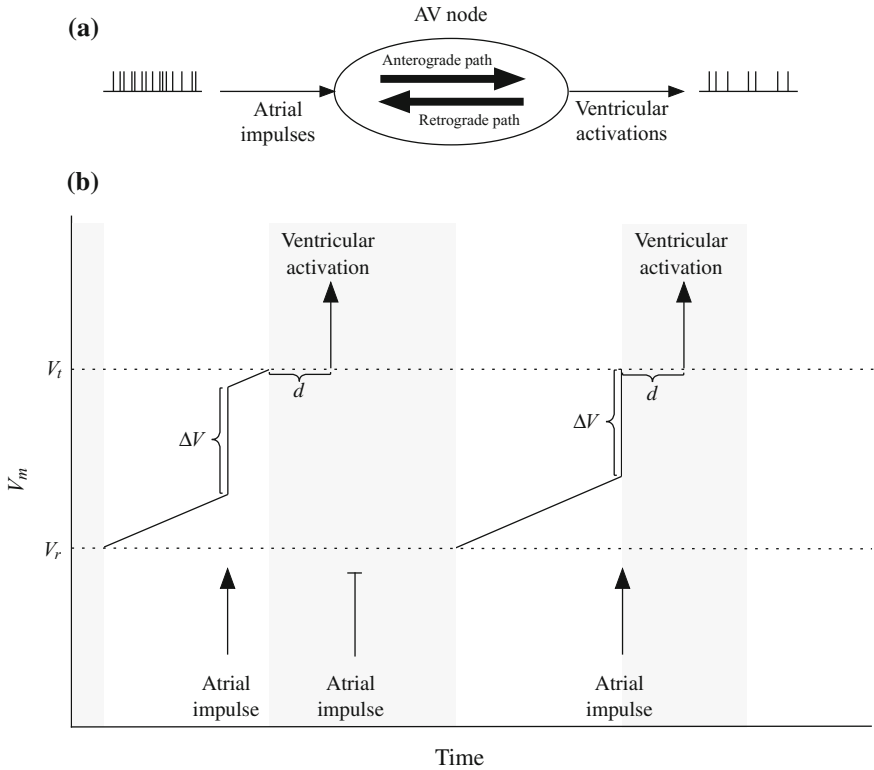
Fig. 7.5 a Schematic representation of the AV node model in [35], and **b** related modeling of the transmembrane potential V_m of the AV node. The resting value V_r can increase spontaneously in a linear fashion as well as by a discrete amount ΔV when an atrial impulse arrives. When V_m exceeds the threshold V_t, an action potential is fired and the AV node becomes refractory for a certain period of time τ'_k (indicated by the grey area). Ventricular activation is associated with a delay d_k, modeled by (7.3). Prolongation of the refractory period due to a blocked atrial impulse is modeled by (7.17)

strength of the atrial impulse,

$$\tau'_k = \tau_k + \tau_{\min} \left(\frac{t_{a,k}}{\tau_k} \right)^{\rho_1} \left(\min \left(1, \frac{\Delta V}{V_t - V_r} \right) \right)^{\rho_2}, \tag{7.17}$$

where τ'_k is the prolonged refractory period and ΔV is the strength of an atrial impulse. The voltages V_t and V_r are defined in Fig. 7.5. The two positive-valued exponents ρ_1 and ρ_2 are model constants.

Figure 7.6 shows two simulated RR series generated using different model parameter settings [35, 39]. The simulation is based on the assumption that atrial impulses arrive to the AV node according to a Poisson process with mean arrival rate λ_a.

The authors stated that the simulation model may provide a quantitative framework to investigating drug effects by fitting their model to experimental data. However,
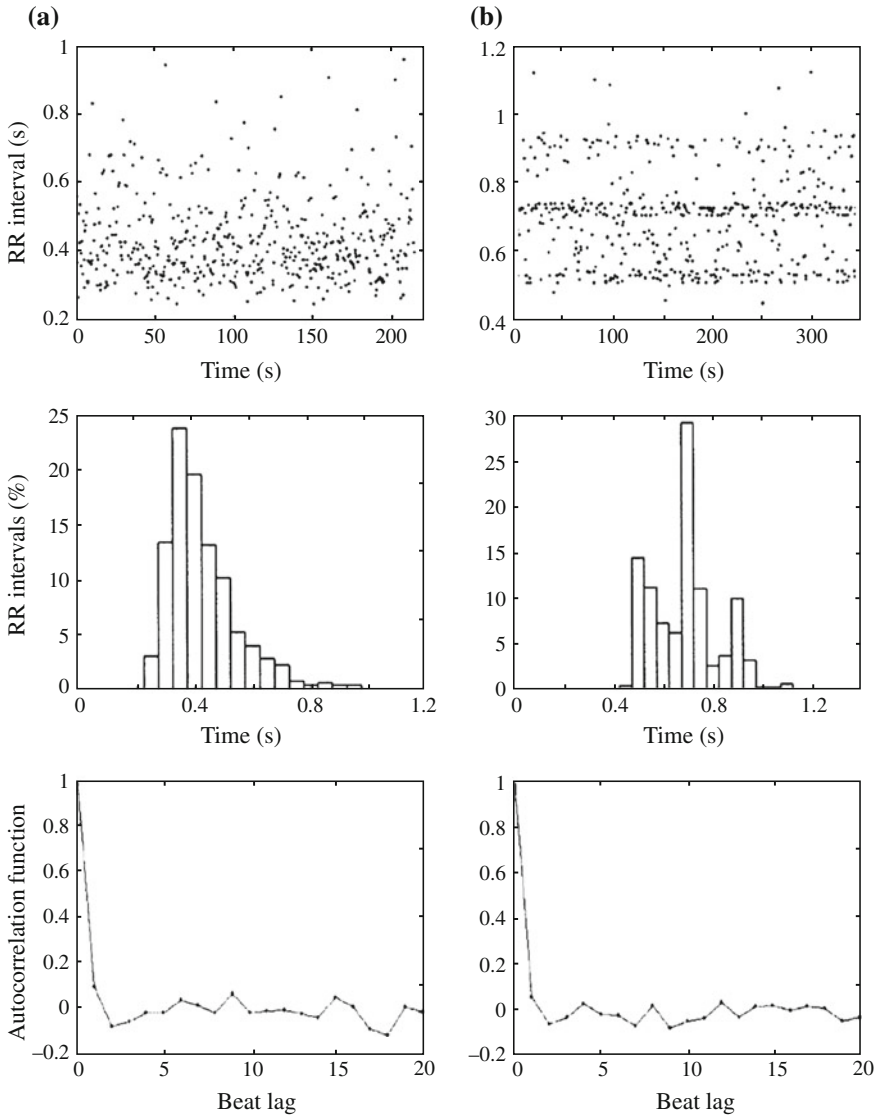
Fig. 7.6 Simulated RR intervals series obtained for two different settings of model parameters [35] (top row), and corresponding (**b**) histogram (middle row), and **c** autocorrelation function (bottom row). The following model parameter values were used: **a** $\lambda_a = 8$ per second, $\Delta V = 20$ mV, $\rho_1 = 10$, $\rho_2 = 10$, and **b** $\lambda_a = 4$ per second, $\Delta V = 10$ mV, $\rho_1 = 10$, $\rho_2 = 10$. (Reprinted from [35] with permission)

no results have so far been published which investigate such effects. The problem of fitting the model to observed data is likely to be challenging since the model involves a large number of parameters.

7.5.5 Modeling of Spatial Dynamics

A radically different approach to modeling is to treat the AV node as a connected graph [42], consisting of a series of interacting nodes, rather than having a lumped structure as the above-described AV node models. An advantage of the graph approach is that it accounts for spatial propagation of atrial impulses in the AV node, implying that phenomena such as concealed conduction and retrograde conduction are intrinsic to the model structure.

The nodes in the graph model propagate impulses, corresponding to action potentials, along the graph edges, see Fig. 7.7. Each node corresponds to a localized part of the AV node with its own conduction delay and refractory period, both quantities depending on the stimulation history of the node. When an impulse arrives at a node, the conduction delay and the refractory period are updated according to (7.3) and (7.16), respectively. Each node has its own dynamics and is characterized by its own recovery time Δt_{RT}, thus differing from the above-described models where the recovery time applies to the whole AV node.

The proposed model consists of 21 nodes, where 10 nodes characterize the fast pathway and 11 the slow pathway. The parameters modeling conduction delay, i.e., d_{min}, α_{max}, and γ_c in (7.3), and refractory period, i.e., τ_{min}, β, and γ_r in (7.16), are identical for all nodes of the slow pathway; the same applies to all nodes of the fast pathway. Hence, the model is defined by 12 parameters. To simulate conduction through the model, it is assumed that the first nodes on the atrial side of the slow and the fast pathways are simultaneously activated. A ventricular activation occurs

Slow pathway

Fast pathway
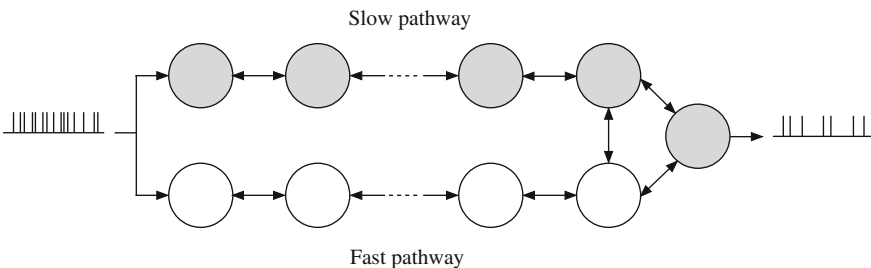
Fig. 7.7 Schematic presentation of the spatial AV node model proposed in [42]. The graph nodes propagate impulses along the edges. Each node is characterized by its own refractory period and conduction delay, both depending on the stimulation history of the node. The full model comprises 21 nodes

when the atrial impulse reaches the rightmost end of the graph, corresponding to the bundle of His.

Simulations were performed using AA intervals determined from electrograms recorded from patients with AF, as well as from simulated AA intervals determined by a Poisson process with mean arrival rate λ_a. A genetic algorithm was used to fit the model by minimizing the difference between simulated RR series and observed RR interval series, obtained from a number of ECG recordings. In the simulations using electrogram-derived series of atrial activations, the difference was quantified by the mean square error of the times of ventricular activations. If simulated AA intervals were used and only the ECG was available, the difference was quantified based on the RR interval histogram. The model could accurately replicate the RR intervals determined from the ECG.

The model fitting was repeated 1000 times for different initial conditions, resulting in 1000 estimates of each parameter for each recording [42]. No unique solution was obtained since several different parameter sets resulted in a similar model fit, however, the ranges of the estimated model parameters were limited. For ECG data, 90% of the estimated values of $\tau_{\min}$ and β were within $\pm 20\%$ of the median value of the estimates, whereas this did not apply to $d_{\min}$ and $\alpha_{\max}$.

7.6 Statistical Modeling of the Atrioventricular Node and Parameter Estimation

In the very first paper dealing with statistical modeling, the AV node was treated as a lumped structure whose behavior represents the temporal and spatial summation of the cellular electrical activity [43]. In that model, briefly described in Sect. 7.6.1, the atrial impulses are assumed to arrive randomly in time at the AV node, modeled by a Poisson process with mean rate λ_a [44]. The conduction time is not explicitly modeled.

Many years later, an improved statistical model was proposed which also accounts for dual AV nodal conduction [45, 46], see Sect. 7.6.2. Since the model parameters can be estimated from the surface ECG, without use of any intracardiac information, noninvasive electrophysiological characterization of the AV node is made possible. In a subsequent study, the model was further improved to incorporate pathway switching, accompanied by more robust parameter estimation [47], see Sect. 7.6.3.

7.6.1 A First Statistical Model of the AV Node

In this statistical model, the AV node is always in one of two states. In the first state, the AV node is absolutely refractory to stimulation by atrial impulses. At the onset of the second state, the transmembrane potential is at its resting value, and increases

spontaneously at a constant rate as well as by a discrete amount ΔV when an atrial impulse arrives. When the transmembrane potential reaches its threshold value V_t as a result of any combination of spontaneous and stepwise depolarization, the AV node fires and a new refractory period is initiated, see Fig. 7.8.

The refractory period is assumed to be rate-dependent, implying that a longer RR interval is followed by a longer refractory period, and vice versa. The relation between refractory period and RR interval is modeled by an exponential function,

$$\tau_n = \tau_\infty \left(1 - \exp\left[-\frac{x_n}{\tau_\infty} \right] \right), \tag{7.18}$$
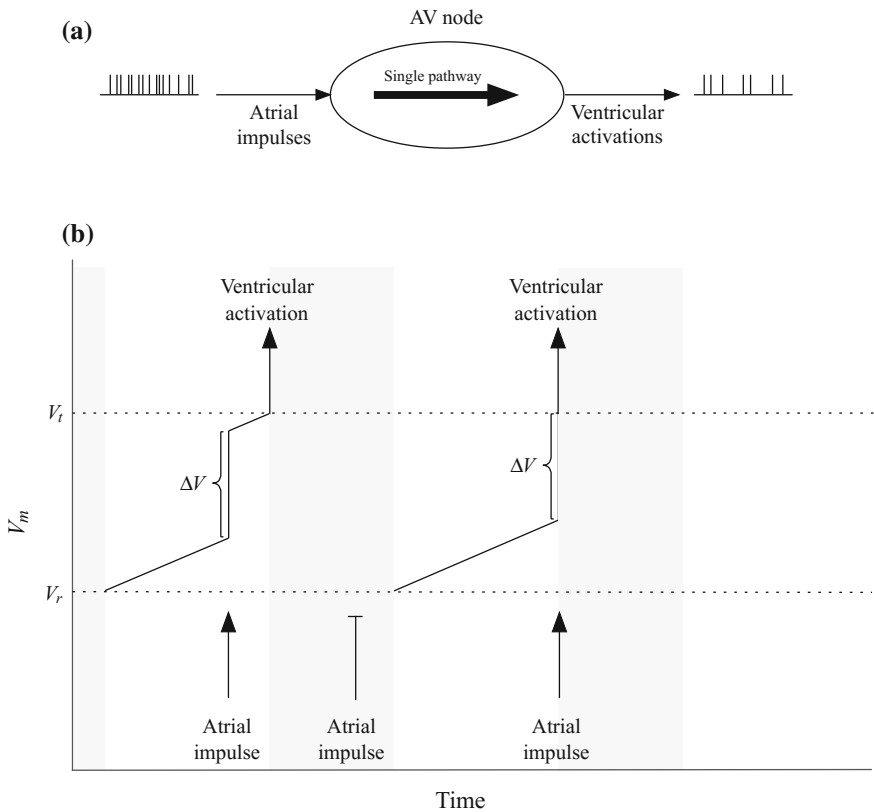
Fig. 7.8 **a** Schematic representation of the AV node model in [43], and **b** related modeling of the transmembrane potential V_m of the AV node. The resting value V_r can increase spontaneously in a linear fashion (defined by the slope v) as well as by a discrete amount ΔV when an atrial impulse arrives. When V_m exceeds the threshold V_t, an action potential is fired and the AV node becomes refractory for a certain period (indicated by the grey area). This model differs from the one in Fig. 7.5 as it does not account for the delay d associated with ventricular activation

where τ_n is the refractory period following the n-th ventricular activation, τ_∞ is the maximal refractory period, and x_n is the RR interval preceding the n-th ventricular activation,

$$x_n = t_{v,n} - t_{v,n-1}. \tag{7.19}$$

The conduction delay is not explicitly modeled.

The model is defined by the following four parameters:

- the mean arrival rate λ_a of atrial impulses,
- the relative amplitude ΔV of atrial impulses,
- the rate v of spontaneous AV depolarization, measured in units of ΔV, and
- the maximal refractory period τ_∞.

Although this model is statistical in nature, no well-established statistical estimation procedure, such as the maximum likelihood (ML) technique, was considered in [43]. Instead, the model parameters were determined using an ad hoc optimization procedure which yielded unphysiological parameter estimates.

7.6.2 Statistical Modeling of Dual AV Nodal Pathways

The improved AV node model accounts for concealed conduction, relative refractoriness, and dual AV nodal pathways [45], see Fig. 7.9. In this model, each atrial impulse is assumed to result in ventricular activation, unless the impulse is blocked by a refractory AV node. The probability of an atrial impulse passing through the AV node depends on the time elapsed since the preceding ventricular activation $t_{v,n-1}$. The refractory period is defined by the sum of a deterministic period τ and a random period, uniformly distributed in the interval $[0, \tau_p]$. The random period models prolongation due to concealed conduction and/or relative refractoriness. All atrial impulses arriving at the AV node before the end of the deterministic period τ are blocked, whereas impulses with arrival time in the interval $[\tau, \tau + \tau_p]$ have linearly increasing likelihood of passing through the AV node. No impulses are blocked if they arrive after $\tau + \tau_p$.

The model accounts for a fast pathway with a longer refractory period, defined by τ_f and $\tau_{f,p}$, and a slow pathway with a shorter refractory period, defined by τ_s and $\tau_{s,p}$ (depending on pathway, the indices "s" and "f" are added to τ and τ_p). In mathematical terms, the refractoriness of the slow pathway is defined by the function $\beta_s(t)$,

$$\beta_s(t) = \begin{cases} 0, & 0 < t < \tau_s, \\ \dfrac{t - \tau_s}{\tau_{s,p}}, & \tau_s \leq t < \tau_s + \tau_{s,p}, \\ 1, & t \geq \tau_s + \tau_{s,p}, \end{cases} \tag{7.20}$$

where, for convenience, t is used instead of $\Delta t_{\mathrm{RT},k}$. The function $\beta_f(t)$ characterizes refractoriness of the fast pathway and is identical to $\beta_s(t)$ except that τ_f and $\tau_{f,p}$
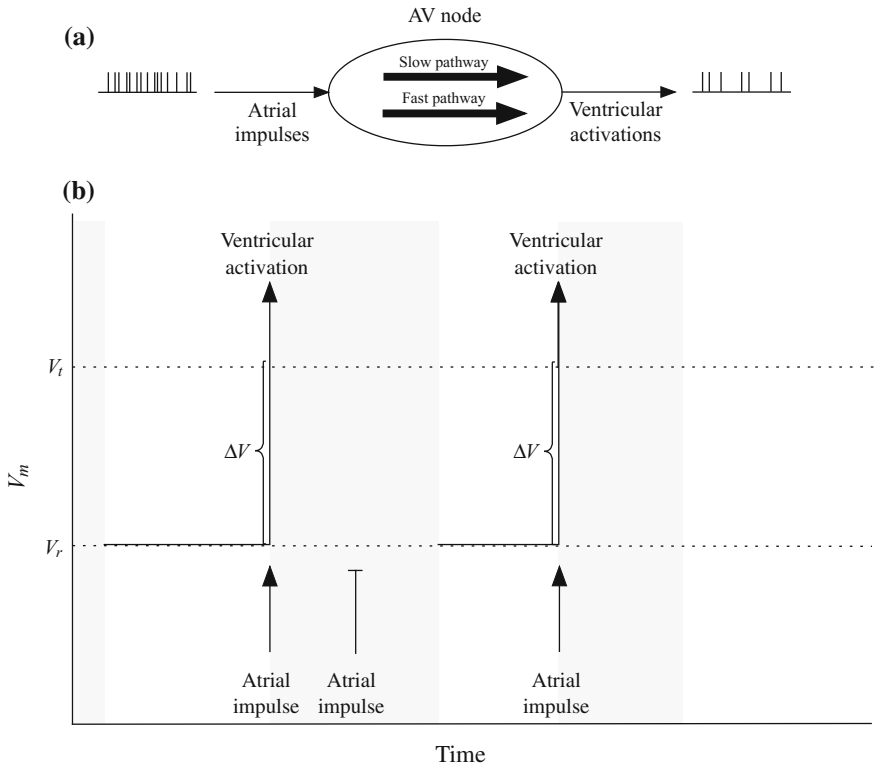
Fig. 7.9 a Schematic representation of the AV node model in [45], and **b** related modeling of the transmembrane potential V_m of the AV node. When an atrial impulse arrives at the AV node, the resting value V_r increases by a discrete amount ΔV which always makes V_m exceed the threshold V_t, an action potential to be fired, and the AV node refractory for a certain period of time (indicated by the grey area)

are substituted for τ_s and $\tau_{s,p}$, respectively. The deterministic part of the refractory periods τ_s and τ_f are assumed to depend linearly on the preceding RR interval x_{n-1}, implying that a longer RR interval is followed by a longer refractory period, and vice versa. Moreover, it is assumed that the AV conduction time is incorporated into $\beta_s(t)$ and $\beta_f(t)$ so that a ventricular activation occurs immediately after a non-blocked atrial impulse.

Since non-blocked atrial impulses are assumed to occur according to an inhomogeneous Poisson process characterized by the intensity function $\lambda_a \beta_s(t)$, the PDF of an RR interval x, related to the slow pathway, is given by [45]

$$p_{x,s}(x) = \lambda_a \beta_s(x) \exp\left[-\int_0^x \lambda_a \beta_s(\tau)d\tau\right], \qquad (7.21)$$

which, after insertion of (7.20), becomes

$$p_{x,s}(x) = \begin{cases} 0, & 0 < x < \tau_s, \\[2ex] \dfrac{\lambda_a(x - \tau_s)}{\tau_{s,p}} \exp\left[-\dfrac{\lambda_a(x - \tau_s)^2}{2\tau_{s,p}}\right], & \tau_s \le x < \tau_s + \tau_{s,p}, \\[2ex] \lambda_a \exp\left[-\dfrac{\lambda_a \tau_{s,p}}{2} - \lambda_a(x - \tau_s - \tau_{s,p})\right], & x \ge \tau_s + \tau_{s,p}. \end{cases} \quad (7.22)$$

The PDF $p_{x,f}(x)$, related to the fast pathway, is obtained by substituting τ_f and $\tau_{f,p}$ for τ_s and $\tau_{s,p}$ in (7.22), respectively.

Conduction through the slow and fast pathways are assumed to occur with probabilities ε and $1 - \varepsilon$, respectively. Assuming that ventricular activations occur according to a Poisson process, the intervals between successive ventricular activations are statistically independent, and the joint probability of the RR intervals $x_0, \ldots, x_{N-1}$ is given by

$$\begin{aligned} p_x(x_0, x_1, \ldots, x_{N-1}) &= \prod_{n=0}^{N-1} p_x(x_n) \\ &= \prod_{n=0}^{N-1} (\varepsilon p_{x,s}(x_n) + (1 - \varepsilon) p_{x,f}(x_n)). \end{aligned} \quad (7.23)$$

The mean arrival rate λ_a is estimated from the f wave signal extracted from the ECG, but corrected to account for atrial refractoriness, using [46]

$$\hat{\lambda}_a = \frac{\lambda_{\mathrm{AF}}}{1 - \delta \lambda_{\mathrm{AF}}}, \quad (7.24)$$

where λ_{AF} is taken as the AFR, estimated from the ECG, and δ is the minimal time interval between successive impulses arriving to the AV node. The five model parameters $\boldsymbol{\theta} = \begin{bmatrix} \varepsilon & \tau_s & \tau_{s,p} & \tau_f & \tau_{f,p} \end{bmatrix}$ are estimated from the observed RR interval series using the ML technique, defined by

$$\hat{\boldsymbol{\theta}} = \arg\max_{\boldsymbol{\theta}} \log p_x(x_0, x_1, \ldots, x_{N-1} | \boldsymbol{\theta}; \hat{\lambda}_a). \quad (7.25)$$

Since no closed-form solution can be found for the estimator $\hat{\boldsymbol{\theta}}$, combined with the fact that the gradient is discontinuous, the multi-swarm particle swarm optimization is used to optimize the log-likelihood function [48, 49]. It should be noted that since τ_s and τ_f depend on the preceding RR interval, the original RR interval series is subject to decorrelation before ML estimation is performed, to better comply with the assumption of statistical independence in (7.23) [45].

The parameters of the single pathway model, i.e., $\begin{bmatrix} \tau & \tau_p \end{bmatrix}^T$, are also estimated. The Bayes information criterion is then used to determine which of the single- and the dual-pathway model is most likely the observed [46].

The block diagram in Fig. 7.10 shows the main signal processing steps required to estimate the model parameters from the ECG. Figure 7.11 illustrates, in histogram form, the RR intervals produced by three different parameter settings of the AV node model.

The AV node model was fitted to clinical data acquired during treatment with different drugs for the purpose of investigating drug-induced changes in AV nodal properties [50–52]. The hypothesis was that the estimates of AV nodal refractory periods would reflect the main changes in AV nodal properties previously reported in studies performed in sinus rhythm and based on invasive data. The effects of tecadenoson and esmolol were investigated in a small cohort of patients [50]. The parameters τ_s and τ_f, accounting for both effective refractory period and conduction interval, were prolonged for both tecadenoson and esmolol [50]. The increase in τ_s and τ_f, observed for both pathways, suggested either prolonged effective refractory
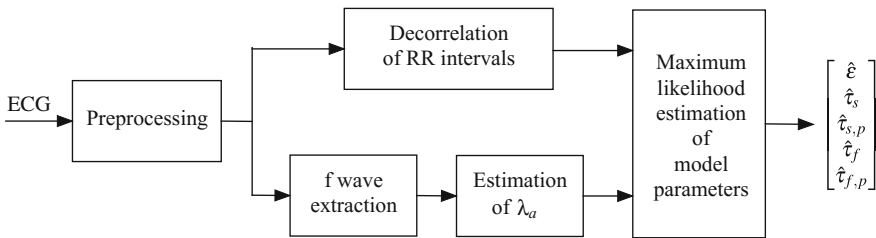
Fig. 7.10 The main signal processing steps required for estimating the AV node model parameters from the ECG
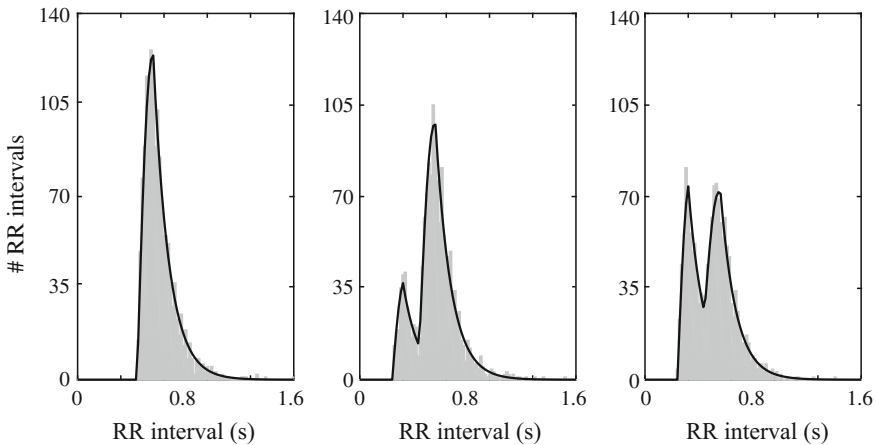
Fig. 7.11 RR interval histogram (area defined by grey bars) and fitted model PDF (solid line) for three different parameter settings. The histograms derive from model data with increasing probability ε of an atrial impulse passing through the slow pathway, set to either 0, 0.25, or 0.5 (left to right); the other model parameters were held constant. (Reprinted from [45] with permission)

period[2] or prolonged AV conduction, or both. In addition, tecadenoson was shown
to affect heart rate but not AFR, suggesting that a decrease in heart rate may be
attributed to that tecadenoson affects the AV node. These results are in agreement
with previous studies demonstrating that tecadenoson prolongs the effective refrac-
tory period of the AV node and slows down its conduction [53], whereas esmolol
prolongs refractoriness and conduction time in both pathways during AV nodal reen-
trant tachycardia [54].

Changes in AV nodal properties were investigated during administration of beta
blockers (carvedilol and metoprolol) and calcium channel blockers (diltiazem and
verapamil) in a controlled setting [52]. For patients with permanent AF, this study
compared the effects of four once-daily drug regimens (metoprolol, diltiazem, ver-
apamil and carvedilol) on heart rate and arrhythmia-related symptoms. While the
results of this study are not directly comparable to previous studies, the changes in
estimated AV nodal properties are in agreement with previous electrophysiological
findings [55–58].

The results suggest that the noninvasively obtained parameter estimates reflect the
expected changes in AV nodal properties for the investigated drugs. Therefore, the
method should be suitable for assessing the drug effect on AV nodal electrophysiology
during AF, especially for antiarrhythmic compounds aimed at rate-control during AF
and tested in clinical trials during initial clinical phases of drug development.

Another application of the AV node model is to analyze data acquired during rest
and head-up tilt ($75°$) from patients with persistent AF. A shortening of the refractory
periods τ_s and τ_f was observed for both pathways during adrenergic activation [59]—
results which are in agreement with earlier reported results [60]. The effect of tilting
on the refractory period of the AV node has not been assessed previously, but invasive
studies have evaluated the effect of vagal tone on AV node refractory periods by either
stimulating the vagal nerve directly [60] or by assessing the effect of vagolytic drugs.

7.6.3 Statistical Modeling of Pathway Switching

A limitation of the statistical model in [45] is the assumption that atrial impulses
arriving between two ventricular activations attempt conduction through the same
pathway, i.e., pathway switching is not allowed. Therefore, another model suitable
for ECG-based estimation of the model parameters was proposed in [47]. Similar to
the model in [45], atrial impulses are assumed to arrive at the AV node according to
a Poisson process with mean arrival rate λ_a. Each impulse attempts to pass through
either the slow or the fast pathway, being blocked according to the time-dependent
functions $\beta_s(t)$ and $\beta_f(t)$ depending on which pathway is chosen. The choice of
pathway is independent of the pathway taken by the preceding atrial impulse. Con-
duction through the slow pathway is attempted with probability ε, and consequently
conduction through the fast pathway is attempted with probability $1 - \varepsilon$.

---

[2]The effective refractory period is defined as the longest nonconducting AA interval.

Since an atrial impulse is assumed to arrive at the AV node according to a Poisson process, the PDF of the arrival time of the first atrial impulse following a ventricular activation is given by [61]

$$p_1(t) = \begin{cases} \lambda_a e^{-\lambda_a t}, & t \geq 0, \\ 0, & t < 0. \end{cases} \tag{7.26}$$

The first impulse attempts conduction through the slow pathway with probability ε, where conduction is characterized by $\beta_s(t)$, defined in (7.20). Hence, the PDF of the arrival time of the first impulse conducted through the slow pathway is given by

$$p_{1,\mathrm{cs}}(t) = \varepsilon \beta_s(t) p_1(t). \tag{7.27}$$

The PDF of the arrival time of the first impulse conducted through the fast pathway $p_{1,\mathrm{cf}}(t)$ is obtained by replacing $\beta_s(t)$ with $\beta_f(t)$ and ε with $1 - \varepsilon$. The notations "cs" and "cf" refers to conduction through the slow and the fast pathway, respectively.

The PDF of the arrival time of the second atrial impulse depends on the arrival time of preceding blocked atrial impulses as well as the time interval between the second and the first atrial impulses, i.e., the AA interval. Since AA intervals are statistically independent in the Poisson model, the PDF of the arrival time of the second atrial impulse following a ventricular activation is given by

$$p_2(t) = \int_0^\infty p_1(t - \rho)(p_{1,\mathrm{bs}}(\rho) + p_{1,\mathrm{bf}}(\rho))d\rho, \tag{7.28}$$

where $p_{1,\mathrm{bs}}(t)$ and $p_{1,\mathrm{bf}}(t)$ denotes the PDF of the arrival time of the first impulse blocked in the slow and the fast pathway, respectively. To account for pathway switching, the second atrial impulse attempts to pass through the slow pathway with probability ε irrespectively of the pathway in which the first impulse was blocked. Hence, $p_{2,\mathrm{cs}}(t)$ and $p_{2,\mathrm{cf}}(t)$ are computed analogously to $p_{1,\mathrm{cs}}(t)$ and $p_{1,\mathrm{cf}}(t)$.

A general expression for recursive computation of the PDF of the arrival times is given by

$$p_{i,\mathrm{cs}}(t) = \varepsilon \beta_s(t) p_i(t), \tag{7.29}$$

$$p_{i,\mathrm{cf}}(t) = (1 - \varepsilon)\beta_f(t) p_i(t), \tag{7.30}$$

$$p_{i,\mathrm{bs}}(t) = \varepsilon(1 - \beta_s(t)) p_i(t), \tag{7.31}$$

$$p_{i,\mathrm{bf}}(t) = (1 - \varepsilon)(1 - \beta_f(t)) p_i(t), \tag{7.32}$$

$$p_{i+1}(t) = \int_0^\infty p_1(t - \rho)(p_{i,\mathrm{bs}}(\rho) + p_{i,\mathrm{bf}}(\rho))d\rho, \tag{7.33}$$

where $p_{i+1}(t)$ denotes the PDF of the arrival time of the $(i + 1)$:st atrial impulse following a ventricular activation, $p_{i,\mathrm{cs}}(t)$ and $p_{i,\mathrm{cf}}(t)$ denote the PDFs of the arrival time of the i-th atrial impulse conducted through the slow pathway and the fast

pathway, respectively, and $p_{i,\text{bs}}(t)$ and $p_{i,\text{bf}}(t)$ denote the corresponding PDFs of blocked atrial impulses.

A conducted atrial impulse is assumed to immediately cause a ventricular activation. Hence, the PDF of the time intervals between ventricular activations, i.e., x_n, is obtained by summing the PDFs of all conducted atrial impulses,

$$p_c(x_n; J) = \sum_{i=1}^{J}(p_{i,\text{cs}}(x_n) + p_{i,\text{cf}}(x_n)), \tag{7.34}$$

where J denotes the maximal number of blocked atrial impulses between successive ventricular activations. This number is chosen so that more than 90% of the conducted atrial impulses are accounted for [47].

When applying the model in [47] to ECG signals, the probability ε of choosing the slow pathway was simply set to 0.5, whereas the remaining model parameters $\boldsymbol{\theta} = \begin{bmatrix} \tau_s & \tau_f & \tau_{s,p} & \tau_{f,p} \end{bmatrix}$ were estimated using the ML technique,

$$\hat{\boldsymbol{\theta}} = \arg\max_{\boldsymbol{\theta}}\left(\sum_{n=0}^{N-1}\log p_c(x_n|\boldsymbol{\theta}; \hat{\lambda}_a)\right), \tag{7.35}$$

where the mean arrival rate λ_a was estimated as described in Sect. 7.6.2.

The ratio of atrial impulses conducted through the slow pathway, defined by

$$\alpha = \frac{\sum_{i=1}^{J}\int_0^\infty p_{i,\text{cs}}(t)dt}{\int_0^\infty p_c,(t; I)dt}, \tag{7.36}$$

can be used to quantify the reliability of the parameter estimates in $\hat{\boldsymbol{\theta}}$. A small α indicates that few impulses are conducted through the slow pathway, and, therefore, $\hat{\tau}_s$ and $\hat{\tau}_{s,p}$ are less reliable. Conversely, a large α indicates that few impulses are conducted through the fast pathway, and, therefore, $\hat{\tau}_f$ and $\hat{\tau}_{f,p}$ are less reliable.

The AV node model has been fitted to each nonoverlapping, 30-min segment of 24-h ECG recordings from 60 patients in permanent AF [47]. Based on results from simulated data, a threshold was applied to α in order to judge whether the estimated model parameters were reliable. Figure 7.12 illustrates how the four parameters characterizing the refractory periods change over a 24 h period, using the models in [45, 47]. It is obvious from Fig. 7.12 that the estimates based on the AV node model in [47] is associated with less variation in $\hat{\tau}_{s,p}$ and $\hat{\tau}_{f,p}$ than is the model in [45]. It should be noted that the model in [47] leads to an unequally sampled series of parameter estimates, since several estimates are omitted because the reliability, determined by α, is judged to be too low.
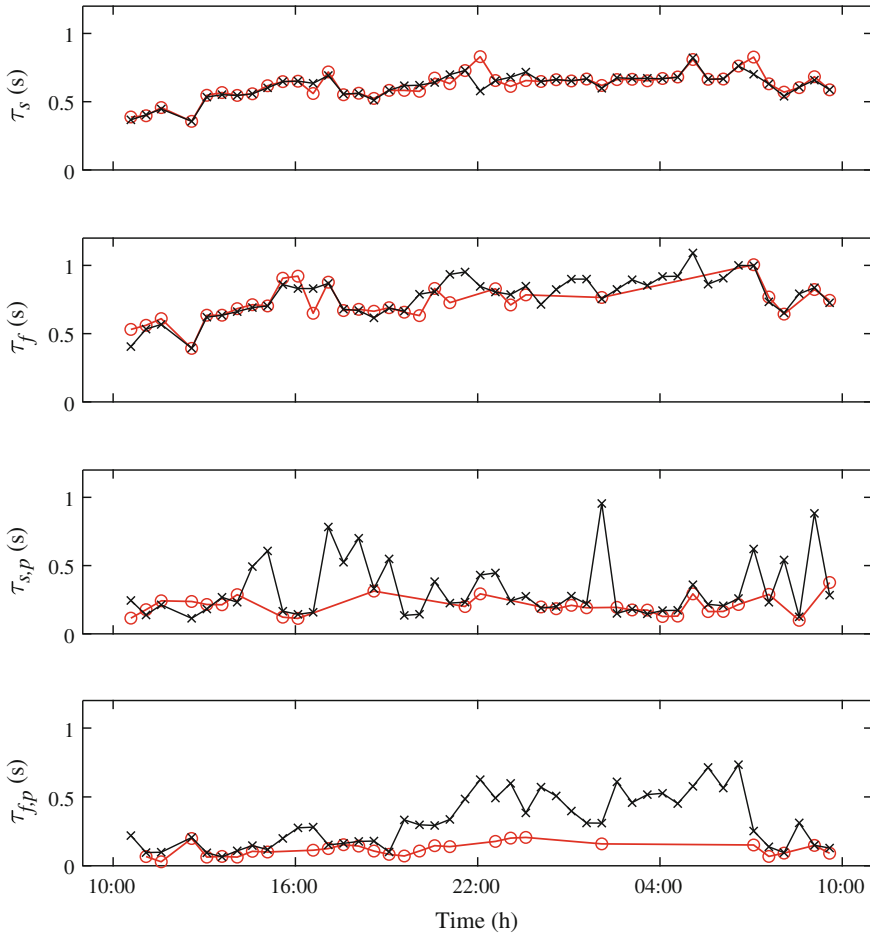
Fig. 7.12 Model parameter estimates obtained from a 24-h ECG recording of a patient with permanent AF, using the models in [47] (red line, "o" markers) and [45] (black line, "x" markers). Successive estimates, indicated by markers, are connected with straight lines (see text for further explanations)

7.7   Comparison of AV Models

The AV node models described in this chapter were developed for different purposes, one purpose being to simulate ventricular activation series resembling those observed during AF and to characterize AV nodal function from intracardiac recordings (Sect. 7.5), another purpose being to characterize AV nodal function from the surface ECG (Sect. 7.6). These purposes are reflected in the structure and complexity of the different models. While the early models embrace two to six parameters [33, 34, 38, 43], the more recent ones, primarily used for simulation and electrogram-based

characterization are considerably more complex, embracing 12 to 16 parameters [35, 36, 42]. The statistical models for ECG-based characterization consist of four to five model parameters which make them better suited for estimation [45, 47].

The AV node models differ in their respective approach to handling the following properties:

- Atrial activation times
- Refractory period
- Conduction delay
- Ventricular activation
- Concealed conduction
- Dual pathways

The *atrial activation times* are usually modeled by a homogenous Poisson process, implying that the AA intervals are exponentially distributed [35, 42, 43, 45, 47]. A Gaussian distribution of the AA intervals has also been proposed [38], although the atrial activation times can no longer be treated as a Poisson process. In the very first statistical model, the mean arrival rate λ_a of the Poisson process assumed an unphysiological value [43]—a problem which was later solved by relating λ_a to the AFR, estimated from the f waves in the ECG [42, 45, 47]. For models where the AV node is characterized using intracardiac information, the atrial activation times are determined by the peaks of the atrial electrogram [33, 34, 36]. Positioning of the electrodes relative to the AV node entrance is particularly important during AF because of the disorganized atrial activity.

From experimental data obtained using a pacing protocol, the effective *refractory period* is known to be dependent on the paced atrial rate [62]. This rate dependence can be modeled in different ways. For example, the refractory period can depend on the preceding RR interval according to an exponential curve defined by the maximal refractory period τ_∞, cf. (7.18) [43]. Another approach is to assume that the refractory period is linearly dependent on the preceding RR interval, calling for decorrelation of the observed RR interval series before parameter estimation can be performed [45, 47]. Yet another approach is to assume that the refractory period is recovery-dependent, i.e., dependent on the time elapsed since the end of the preceding refractory period according to an exponential curve modeled by three parameters: the minimal refractory period $\tau_{\min}$, the maximal prolongation β, and the time constant γ_r of the exponential refractory curve, cf. (7.16) [35, 42]. In some models, the rate dependence of the refractory period is not explicitly modeled [33, 34, 36, 38].

The *conduction delay* is an important property of the AV node during normal sinus rhythm, known to be dependent on the paced atrial rate [62]. The AV nodal conduction delay may be incorporated in the refractory period so that its dynamics is not explicitly modeled [43, 45, 47]. Alternatively, the conduction delay can be made dependent on the recovery time, where recovery dependence is modeled by an exponential curve defined by three model parameters: the minimal conduction delay $d_{\min}$, the maximal prolongation $\alpha_{\max}$, and the time constant γ_c of the exponential conduction curve, cf. (7.3) [33–35, 42]. A similar approach was considered in [36],

although the maximal prolongation and the time constant of the conduction curve were assumed to depend on the preceding conduction delay.

In most models, ventricular activation is directly linked to the arrival of one atrial impulse. Each atrial impulse is assumed to result in a *ventricular activation*, unless it is blocked due to AV nodal refractoriness. However, more than one atrial impulse may be needed to cause a ventricular activation [35, 43]. The AV node may also fire spontaneously.

Concealed conduction is incorporated in the models in different ways. For each blocked impulse, the refractory period can be incremented by a fixed [33] or random time [34]. The refractory period prolongation can depend on the timing of the blocked impulse [38], or on both the timing and the strength of the blocked impulse [35]. Blocked impulses can alter the conduction time of the following impulse, so that a longer AA interval results in a longer conduction delay [36]. Concealed conduction can also be disregarded, assuming a refractory period which is not influenced by blocked impulses [43]. The refractory period prolongation caused by each blocked impulse is not always explicitly modeled, but concealed conduction is modeled by a random, uniformly distributed prolongation of the refractory period [45, 47]. Concealed conduction can also be an intrinsic feature of the chosen model structure [42].

The earlier models [33–35, 38, 43] did not account for *dual pathways* of the AV node, while the more recent models account for separate conduction time [36, 42] and refractory period [42, 45, 47] of the two pathways.

The model in [43] was fitted to observed RR series using an ad hoc procedure. For some models, no attempts have been made at all to fit the models to observed data [35, 38]. The models proposed for characterization of AV nodal function based on intracardiac recordings were fitted using a grid search to find the minimum error between observed and simulated RR intervals, given the observed AA intervals as input [33, 34, 42]. The model parameters in [36] were assessed by fitting data obtained using

Table 7.1 Comparison of atrioventricular node models with respect to structure and atrial impulse assumptions. The models are listed in chronological order

Model proposed by	Model parameters	Parameter estimation	Atrial impulses	Impulses required
Cohen et al. [43]	4	No	Poisson	≥ 0
Jorgensen et al. [33]	6	Ad hoc	Invasive data	1
Rashidi and Khodarahmi [38]	2	No	Gaussian	1
Mangin et al. [34]	6	Ad hoc	Invasive data	1
Lian et al. [35]	16	No	Poisson	≥ 0
Climent et al. [36]	18	Ad hoc	Invasive data	1
Corino et al. [45]	6	ML	Poisson	1
Henriksson et al. [47]	5	ML	Poisson	1
Wallman and Sandberg [42]	12	Ad hoc	Poisson	1

Table 7.2 Comparison of atrioventricular node models with respect to various electrophysiological properties. The functional dependence of the refractory period is indicated, where x_n is the preceding RR interval, and $\Delta t_{RT,k}$ is the AV nodal recovery time, cf. (7.4)

Model proposed by	Conduction delay	Refractory period	Concealed conduction	Dual pathways
Cohen et al. [43]	No	x_n	No	No
Jorgensen et al. [33]	Yes	Fixed	Fixed increment	No
Rashidi and Khodarahmi [38]	No	Fixed	Timing	No
Mangin et al. [34]	Yes	Fixed	Random increment	No
Lian et al. [35]	yes	$\Delta t_{RT,k}$	Timing and strength	No
Climent et al. [36]	Yes	No	Timing	Yes
Corino et al. [45]	No	x_n	Random	Yes
Henriksson et al. [47]	No	x_n	Random	Yes
Wallman and Sandberg [42]	Yes	$\Delta t_{RT,k}$	Intrinsic	Yes

a dedicated pacing protocol. For ECG-based characterization of AV nodal function during AF, the mean arrival rate of atrial impulses is estimated from an extracted f wave signal [42, 45, 47]; the remaining model parameters are estimated from an RR interval series using ML estimation [45, 47].

Tables 7.1 and 7.2 provides a comparison of AV node models described in this chapter and their respective properties.

References

1. K.M. Stein, J. Walden, N. Lippman, B.B. Lerman, Ventricular response in atrial fibrillation: random or deterministic? Am. J. Physiol. **277**, H452–458 (1999)
2. V.D.A. Corino, R. Sassi, L.T. Mainardi, S. Cerutti, Signal processing methods for information enhancement in atrial fibrillation: spectral analysis and non-linear parameters. Biomed. Signal Process. Control **1**, 271–281 (2006)
3. P. Kirchhof, S. Benussi, D. Kotecha, A. Ahlsson, D. Atar, B. Casadei, M. Castella, H.C. Diener, H. Heidbuchel, J. Hendriks, G. Hindricks, A.S. Manolis, J. Oldgren, B.A. Popescu, U. Schotten, B. Van Putte, P. Vardas, S. Agewall, J. Camm, G. Baron Esquivias, W. Budts, S. Carerj, F. Casselman, A. Coca, R. De Caterina, S. Deftereos, D. Dobrev, J.M. Ferro, G. Filippatos, D. Fitzsimons, B. Gorenek, M. Guenoun, S.H. Hohnloser, P. Kolh, G.Y. Lip, A. Manolis, J. McMurray, P. Ponikowski, R. Rosenhek, F. Ruschitzka, I. Savelieva, S. Sharma, P. Suwalski, J.L. Tamargo, C.J. Taylor, I.C. Van Gelder, A.A. Voors, S. Windecker, J.L. Zamorano, K. Zeppenfeld, 2016 ESC guidelines for the management of atrial fibrillation developed in collaboration with EACTS. Eur. Heart J. **37**, 2893–2962 (2016)
4. L. Sörnmo, P. Laguna, *Bioelectrical Signal Processing in Cardiac and Neurological Applications* (Elsevier (Academic Press), Amsterdam, 2005)

5. B. Frey, G. Heinz, T. Binder, M. Wutte, B. Schneider, H. Schmidinger, H. Weber, R. Pacher, Diurnal variation of ventricular response to atrial fibrillation in patients with advanced heart failure. Am. Heart J. **129**, 58–65 (1995)
6. K.M. Stein, J.S. Borer, C. Hochreiter, R.B. Devereux, P. Kligfield, Variability of the ventricular response in atrial fibrillation and prognosis in chronic nonischemic mitral regurgitation. Am. J. Cardiol. **74**, 906–911 (1994)
7. R. Sassi, S. Cerutti, F. Lombardi, M. Malik, H.V. Huikuri, C.-K. Peng, G. Schmidt, Y. Yamamoto, B. Gorenek, G.Y. Lip, G. Grassi, G. Kudaiberdieva, J.P. Fisher, M. Zabel, R. Macfadyen, Advances in heart rate variability signal analysis: joint position statement by the e-Cardiology ESC Working Group and the European Heart Rhythm Association co-endorsed by the Asia Pacific Heart Rhythm Society. Europace **17**, 1341–1353 (2015)
8. A. Porta, G. Baselli, D. Liberati, N. Montano, C. Cogliati, T. Gnecchi-Ruscone, A. Malliani, S. Cerutti, Measuring regularity by means of a corrected conditional entropy in sympathetic outflow. Biol. Cybern. **78**, 71–78 (1998)
9. A. Yamada, J. Hajano, S. Sakata, A. Okada, S. Mukai, N. Ohte, G. Kimura, Reduced ventricular response irregularity is associated with increased mortality in patients with chronic atrial fibrillation. Circulation **102**, 300–306 (2000)
10. R. Vazquez, A. Bayes-Genis, I. Cygankiewicz, D. Pascual-Figal, L. Grigorian-Shamagian, R. Pavon, J. Gonzalez-Juanatey, J. Cubero, L. Pastor, J. Ordonez-Llanos, J. Cinca, A. de Luna, MUSIC investigators, The MUSIC risk score: a simple method for predicting mortality in ambulatory patients with chronic heart failure. Eur. Heart J. **30**, 1088–1096 (2009)
11. J.T. Rich, J.G. Neely, R.C. Paniello, C.C.J. Voelker, B. Nussenbaum, E.W. Wang, A practical guide to understanding Kaplan–Meier curves. Otolaryngol. Head Neck. Surg. **143**, 331–336 (2010)
12. I. Cygankiewicz, V.D.A. Corino, R. Vazquez, A. Bayes-Genis, L.T. Mainardi, W. Zareba, A. Bayes de Luna, P. G. Platonov, Reduced irregularity of ventricular response during atrial fibrillation and long-term outcome in patients with heart failure. Am. J. Cardiol. **116**, 1071–1075 (2015)
13. V.D.A. Corino, F. Holmqvist, L.T. Mainardi, P.G. Platonov, Beta-blockade and A1-adenosine receptor agonist effects on atrial fibrillatory rate and atrioventricular conduction in patients with atrial fibrillation. Europace **16**, 587–594 (2014)
14. V.D.A. Corino, I. Cygankiewicz, L.T. Mainardi, M. Stridh, W. Zareba, R. Vasquez, A. Bayes de Luna, P.G. Platonov, Association between atrial fibrillatory rate and heart rate variability in patients with atrial fibrillation and congestive heart failure. Ann. Noninvasive Electrophysiol. **18**, 41–50 (2013)
15. V.D.A. Corino, S.R. Ulimoen, S. Enger, L.T. Mainardi, A. Tveit, P.G. Platonov, Rate-control drugs affect variability and irregularity measures of RR intervals in patients with permanent atrial fibrillation. J. Cardiovasc. Electrophysiol. **26**, 137–141 (2015)
16. L.T. Mainardi, A. Porta, G. Calcagnini, P. Bartolini, A. Michelucci, S. Cerutti, Linear and non-linear analysis of atrial signals and local activation period series during atrial-fibrillation episodes. Med. Biol. Eng. Comput. **39**, 249–254 (2001)
17. V.D.A. Corino, P.G. Platonov, S. Enger, A. Tveit, S.R. Ulimoen, Circadian variation of variability and irregularity of heart rate in patients with permanent atrial fibrillation: relation to symptoms and rate control drugs. Am. J. Physiol. Heart Circ. Physiol. **309**, H2152–H2157 (2015)
18. C. Bingham, B. Arbogast, C.C. Guillaume, J.K. Lee, F. Halberg, Inferential statistical methods for estimating and comparing cosinor parameters. Chronobiologia **9**, 397–439 (1982)
19. R. Refinetti, G. Cornélissen, F. Halberg, Procedures for numerical analysis of circadian rhythms. Biol. Rhythm Res. **38**, 275–325 (2007)
20. J. Billette, R.A. Nadeau, F. Roberge, Relation between the minimum RR interval during atrial fibrillation and the functional refrectory period of the AV junction. Cardiovasc. Res. **8**, 347–351 (1974)
21. M. Talajic, D. Papadatos, C. Villemaire, L. Glass, S. Nattel, A unified model of atrioventricular nodal conduction predicts dynamic changes in Wenckebach periodicity. Circ. Res. **68**, 1280–1293 (1991)

22. L. Toivonen, A. Kadish, W. Kou, F. Morady, Determinants of the ventricular rate during atrial fibrillation. J. Am. Coll. Cardiol. **16**, 1194–1200 (1990)
23. A. Khand, A. Rankin, J. Cleland, I. Gemmell, E. Clark, P. Macfarlane, The assessment of autonomic function in chronic atrial fibrillation: description of a non-invasive technique based on circadian rhythm of atrioventricular nodal functional refractory period. Europace **8**, 927–934 (2006)
24. J. Hayano, S. Sakata, A. Okada, S. Mukai, T. Fujinami, Circadian rhythms of atrioventricular conduction properties in chronic atrial fibrillation with and without heart failure. J. Am. Coll. Cardiol. **31**, 158–166 (1998)
25. M. Talajic, M. Nayebpour, W. Jing, S. Nattel, Frequency dependent effects of diltiazem on the atrioventricular node during experimental atrial fibrillation. Circulation **80**, 380–389 (1989)
26. M.P. van den Berg, T. van Noord, J. Brouwer, J. Haaksma, D.J. van Veldhuisen, H.J. Crijns, I.C. van Gelder, Clustering of RR intervals predicts effective electrical cardioversion for atrial fibrillation. J. Cardiovasc. Electrophysiol. **15**, 1027–1033 (2004)
27. A. Climent, M. de la Salud Guillem, D. Husser, F. Castells, J. Millet, A. Bollmann, Poincaré surface profiles of RR intervals: a novel noninvasive method for the evaluation of preferential AV nodal conduction during atrial fibrillation. IEEE Trans. Biomed. Eng. **56**, 433–442 (2009)
28. M. Masè, L. Glass, M. Disertori, F. Ravelli, AV synchrogram: a novel approach to quantifying atrioventricular coupling during atrial arrhythmias. Biomed. Signal Process. Control **8**, 1008–1016 (2013)
29. M. Masè, M. Marini, M. Disertori, F. Ravelli, Dynamics of AV coupling during human atrial fibrillation: role of atrial rate. Am. J. Physiol. Heart Circ. Physiol. **309**, H198–H205 (2015)
30. M. Masè, M. Disertori, M. Marini, F. Ravelli, Characterization of rate and regularity of ventricular response during atrial tachyarrhythmias. Insight on atrial and nodal determinants. Physiol. Meas. **38**, 800–818 (2017)
31. J. Sun, F. Amellal, L. Glass, J. Billette, Alternans and period doubling bifurcations in atrioventricular nodal conduction. J. Theor. Biol. **173**, 79–91 (1995)
32. F.L. Meijler, J. Jalife, J. Beaumont, D. Vaidya, AV nodal function during atrial fibrillation: the role of electrotonic modulation of propagation. J. Cardiovasc. Electrophysiol. **7**, 843–861 (1996)
33. P. Jørgensen, C. Schäfer, P.G. Guerra, M. Talajic, S. Nattel, L. Glass, A mathematical model of human atrioventricular nodal function incorporating concealed conduction. Bull. Math. Biol. **64**, 1083–1099 (2002)
34. L. Mangin, A. Vinet, P. Page, L. Glass, Effects of antiarrhythmic drug therapy on atrioventricular nodal function during atrial fibrillation in humans. Europace **7**, S71–S82 (2005)
35. J. Lian, D. Müssig, V. Lang, Computer modeling of ventricular rhythm during atrial fibrillation and ventricular pacing. IEEE Trans. Biomed. Eng. **53**, 1512–1520 (2006)
36. A. Climent, M. Guillem, Y. Zhang, J. Millet, T. Mazgalev, Functional mathematical model of dual pathway AV nodal conduction. Am. J. Physiol. Heart Circ. Physiol. **300**, H1393–1401 (2011)
37. Y. Zhang, S. Bharati, K. Mowrey, T. Mazgalev, His electrogram alternans reveal dual atrioventricular nodal pathway conduction during atrial fibrillation: the role of slow-pathway modification. Circulation **107**, 1059–1065 (2003)
38. A. Rashidi, I. Khodarahmi, Nonlinear modeling of the atrioventricular node physiology in atrial fibrillation. J. Theor. Biol. **232**, 545–549 (2005)
39. J. Lian, D. Müssig, Heart rhythm and cardiac pacing: an integrated dual-chamber heart and pacer model. Ann. Biomed. Eng. **37**, 64–81 (2009)
40. J. Lian, D. Müssig, V. Lang, Ventricular rate smoothing for atrial fibrillation: a quantitative comparison study. Europace **9**, 506–513 (2007)
41. J. Lian, D. Müssig, V. Lang, On the role of ventricular conduction time in rate stabilization for atrial fibrillation. Europace **9**, 289–293 (2007)
42. M. Wallman, F. Sandberg, Characterisation of human AV-nodal properties using a network model. Med. Biol. Eng. Comput. **56**, 247–259 (2018)

43. R.J. Cohen, R.D. Berger, T. Dushane, A quantitative model for the ventricular response during atrial fibrillation. IEEE Trans. Biomed. Eng. **30**, 769–780 (1983)
44. R.E. Goldstein, G.O. Barnett, A statistical study of the ventricular irregularity of atrial fibrillation. Comput. Biomed. Res. **1**, 146–161 (1967)
45. V.D.A. Corino, F. Sandberg, L.T. Mainardi, L. Sörnmo, An atrioventricular node model for analysis of the ventricular response during atrial fibrillation. IEEE Trans. Biomed. Eng. **58**, 3386–3395 (2011)
46. V.D.A. Corino, F. Sandberg, F. Lombardi, L.T. Mainardi, L. Sörnmo, Atrioventricular nodal function during atrial fibrillation: Model building and robust estimation. Biomed. Signal Process. Control **8**, 1017–1025 (2013)
47. M. Henriksson, V.D.A. Corino, L. Sörnmo, F. Sandberg, A statistical atrioventricular node model accounting for pathway switching during atrial fibrillation. IEEE Trans. Biomed. Eng. **63**, 1842–1849 (2016)
48. F. Van den Bergh, A.P. Engelbrecht, A cooperative approach to particle swarm optimization. IEEE Trans. Evolutionary Comput. **8**, 225–239 (2004)
49. B. Niu, X. Zhu, Y. He, H. Wu, MCPSO: a multi-swarm cooperative particle swarm optimize. Appl. Math. Comput. **2**, 1050–1062 (2007)
50. V.D.A. Corino, F. Sandberg, L.T. Mainardi, P.G. Platonov, L. Sörnmo, Noninvasive assessment of atrioventricular nodal function: effect of rate-control drugs during atrial fibrillation. Ann. Noninvasive Electrocardiol. **20**, 534–541 (2015)
51. V.D.A. Corino, F. Sandberg, P.G. Platonov, L.T. Mainardi, S.R. Ulimoen, S. Enger, A. Tveit, and L. Sörnmo, Non-invasive evaluation of the effect of metoprolol on the atrioventricular node during permanent atrial fibrillation. Europace **16** iv129–iv134 (2014)
52. F. Sandberg, V.D.A. Corino, L.T. Mainardi, S. Ulimoen, S. Enger, A. Tveit, P.G. Platonov, L. Sörnmo, Non-invasive assessment of beta blockers and calcium channel blockers on the av node during permanent atrial fibrillation. J. Electrocardiol. **48**, 861–866 (2015)
53. E.N. Prystowsky, I. Niazi, A. Curtis, D.J. Wilber, T. Bahnson, K. Ellenbogen, A. Dhala, D.M. Bloomfield, M. Gold, A. Kadish, R.I. Fogel, M.D. Gonzalez, L. Belardinelli, R. Shreeniwas, A.A. Wolff, Termination of paroxysmal supraventricular tachycardia by tecadenoson (CVT-510), a novel A1-adenosine receptor agonist. J. Am. Coll. Cardiol. **42**, 1098–1102 (2003)
54. F. Philippon, V.P. Plumb, G.N. Kay, Differential effect of esmolol on the fast and slow AV nodal pathways in patients with AV nodal reentrant tachycardia. J. Cardiovasc. Electrophysiol. **5**, 810–817 (1994)
55. F.E. Marchlinski, A.E. Buxton, H.L. Waxman, M.E. Josephson, Electrophysiologic effects of intravenous metoprolol. Am. Heart J. **107**, 1125–1131 (1984)
56. T. Horio, S. Ito, M. Aoyama, Y. Takeda, H. Suzumura, K. Nakata, Y. Yamada, S. Suzuki, T. Fukutomi, I.M, Effect of carvedilol on atrioventricular conduction in the ischemic heart. Eur. J. Pharmacol. **412**, 145–153 (2001)
57. H. Shiina, A. Sugiyama, A. Takahara, Y. Satoh, K. Hashimoto, Comparison of the electropharmacological effects of verapamil and propranolol in the halothane-anesthetized in vivo canine model under monophasic action potential monitoring. Jpn. Circ. J. **64**, 777–782 (2000)
58. M. Talajic, R. Lemery, D. Roy, C. Villemaire, R. Cartier, B. Coutu, S. Nattel, Rate-dependent effects of diltiazem on human atrioventricular nodal properties. Circulation **86**, 870–877 (1992)
59. V.D.A. Corino, F. Sandberg, F. Lombardi, L.T. Mainardi, L.Sörnmo, Statistical modeling of atrioventricular nodal function during atrial fibrillation focusing on the refractory period estimation, in *Biomedical Engineering Systems and Technologies* ed. by M. Fernández-Chimeno et al., vol. 452, (Springer, Heidelberg, 2014) pp. 258–268
60. M. Nayebpour, M. Talajic, C. Villemaire, S. Nattel, Vagal modulation of the rate-dependent properties of the atrioventricular node. Circ. Res. **67**, 1152–1166 (1990)
61. S.M. Ross, *Introduction to Probability Models*, 11th edn. (Academic Press, 2014)
62. J. Billette, R. Tadros, Integrated rate-dependent and dual pathway AV nodal functions: principles and assessment framework. Am. J. Physiol. Heart. Circ. Physiol. **306**, H173–183 (2014)